CO Oxidation over AuPd(100) from Ultrahigh Vacuum to Near-Atmospheric Pressures: CO Adsorption-Induced Surface Segregation and Reaction Kinetics

Feng Gao, Yilin Wang, and D. Wayne Goodman*

Department of Chemistry, Texas A&M University, P.O. Box 30012, College Station, Texas 77842-3012

Received: June 5, 2009; Revised Manuscript Received: July 7, 2009

Polarization-modulation infrared reflection absorption spectroscopy (PM-IRAS) is used to study CO adsorption on AuPd(100) surfaces, one well-annealed such that contiguous Pd sites do not initially exist and a second ion sputtered such that contiguous Pd sites are exposed. At CO pressures $\leq 1 \times 10^{-3}$ Torr, Pd segregation to the surface is found; however, it is not sufficient to form contiguous Pd sites on the well-annealed sample. At CO pressures higher than ~0.1 Torr, Pd segregation becomes greatly enhanced such that contiguous Pd sites form. Isosteric heats of adsorption of CO on Au sites and isolated Pd sites are measured to be 69 and 84 kJ/mol, respectively. The CO heat of adsorption on contiguous Pd sites is found to lie between these values. The CO oxidation reaction, monitored using both PM-IRAS and reaction kinetic measurements, occurs only on surfaces with contiguous Pd sites, due to the fact that O_2 dissociation takes place exclusively on these sites. The surface composition and distribution can be tuned by varying the sample temperature, reactant pressure, and compositions, thus affecting the rate of CO_2 formation. The extremely high reaction rate at relatively low temperatures is attributed to the greatly reduced binding energy of CO with the surface such that CO inhibition, a factor that causes low reaction rate on pure Pd at these temperatures, does not exist with the alloy surface.

1. Introduction

Silica-supported Pd−Au bimetallic catalysts promoted with potassium acetate are commercially used in the synthesis of vinyl acetate.[1−12] Pd−Au alloys also catalyze other important reactions, for example, the selective oxidation of alcohols to aldehydes or ketones and H_2O_2 synthesis.[13−16] Very recent U.S. patents, using PdAu alloy in combination with other precious metals (Pt, PtPd alloy, PtBi alloy, etc.) as engine exhaust catalysts, describe catalytic applications that exhibit substantially reduced CO and hydrocarbon emission.[17] The unique catalytic properties of Pd−Au alloys have stimulated numerous studies on Pd−Au model systems.

Primarily three types of model Pd−Au catalysts have been developed: (1) bulk alloys with specific Pd/Au stoichiometries, for example, PdAu and Pd_3Au, (2) thin film surface alloys prepared by the deposition of Pd onto a single crystal of Au or vise versa,[10−12,18,19] and (3) Pd and Au thin films synthesized by their deposition onto a refractory metal substrate, for example, Mo(110).[20,21] Methods 2 and 3 offer considerable flexibility in varying the surface composition simply by varying the deposition and annealing and thus are ideal methods for studying the structure and composition of *bare* alloy surfaces. However, in studying adsorbate-induced changes in surface composition and structure, method 2 is problematic since this method only has a single metal in the bulk whereas method 3 has no bulk metal reservoir at all. In this sense, the surface of a bulk alloy is advantageous for segregation studies. Previous studies have shown a general trend of surface segregation where the more reactive alloy component forms stronger chemical bond with the adsorbate and thus preferentially segregates to the surface.[22−27]

In a very recent communication we reported CO oxidation over a AuPd(100) single-crystal surface at both ultrahigh vacuum (UHV) and near-atmospheric pressures.[28] AuPd(100) is a good choice for the study since this substrate has equal amounts of Pd and Au in the bulk and thus is ideal for segregation investigations. It was discovered that CO pressures higher than ~0.1 Torr are needed to segregate a sufficient amount of Pd to the surface to form contiguous Pd sites, which are indispensable in O_2 dissociation. The explanation for this behavior is that Au is involved in the surface reaction where $O_{(ads)}$ is formed on contiguous Pd sites and then spills over to Au sites where CO is adsorbed and oxidation occurs.[28] This reaction pathway is likely to be important at relatively low temperatures (<400 K) since the weak interaction between CO and Au precludes CO adsorption on Au sites at elevated temperatures. There appears to be only one other fundamental study in the literature dealing with elevated pressure CO oxidation reaction using Pd−Au single crystal as a model catalyst.[29] This study, however, used reactants with extremely high O_2/CO ratios (100 and 200), thus precluding a general picture to be obtained. In the current study, we present CO oxidation kinetics coupled with in situ spectroscopic investigations over AuPd(100) with further details. The implications of this study to important industrial processes, e.g., vinyl acetate synthesis and catalytic emission control, are also discussed.

2. Experimental Section

Polarization-modulation infrared reflection absorption spectroscopy (PM-IRAS) was the primary tool used in this study to investigate CO adsorption on AuPd(100). The experimental apparatus has been described in detail previously.[30−32] Briefly, the apparatus consists of an ultrahigh vacuum (UHV) section equipped with Auger spectroscopy (AES), low-energy electron diffraction (LEED), a UTI 100 mass spectrometer (QMS), and

* To whom correspondence should be addressed. Phone: 979-845-0214. Fax: 979-845-6822. E-mail: goodman@mail.chem.tamu.edu.

10.1021/jp9053132 CCC: $40.75
Published on Web 07/27/2009

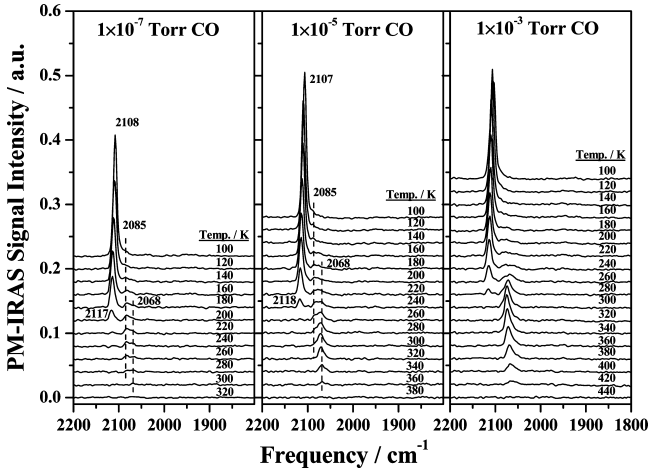

Figure 1. PM-IRAS spectra of CO on a well-annealed AuPd(100) sample as a function of temperature. Sample temperatures are marked adjacent to each spectrum. Spectra acquired at a CO pressure of (left) 1×10^{-7}, (middle) 1×10^{-5}, and (right) 1×10^{-3} Torr.

a high-pressure reaction cell. The AuPd(100) bulk alloy single crystal, purchased from Matek, was cleaned by repeated ion sputtering at room temperature, followed by annealing at 800 K for 20−30 min.[33] The sample cleanliness was verified by AES. The annealing process allowed an equilibrium concentration of surface Pd and Au to be reached. A recent low-energy ion scattering spectroscopy (LEISS) study has revealed that following this treatment, the surface consists of ∼10% of Pd and ∼90% of Au.[33] PM-IRAS measurements were carried out using a Bruker Equinox 55 FTIR spectrometer coupled with a polarization modulator to subtract infrared signals arising from gas-phase absorption. This method allows in situ measurements of surface species over a wide range of pressures from UHV to atmospheric. Two methods were used to study CO oxidation kinetics: (i) low pressure kinetic measurements ($P \leq 10^{-3}$ Torr) were carried out under steady-state flow conditions by backfilling the UHV chamber with the desired gas mixture and monitoring the CO_2 (44 amu) and CO (28 amu) mass spectrometer signals (correcting for fragmentation and sensitivity at these two masses) and (ii) high-pressure kinetic measurements ($P \geq 0.1$ Torr) were conducted in a batch mode using a high-pressure cell (∼1.0 L) attached to but decoupled from the UHV chamber. In the latter case, reaction rates were derived by postreaction analysis of the gas-phase composition using the QMS. CO conversion was kept below 10% to ensure the acquisition of differential reaction rates.

C.P. grade CO (>99.5%, Matheson Tri-Gas) was further purified by passing through 4 A molecular sieve and a liquid nitrogen-cooled trap to remove metal carbonyl impurities. Ultrahigh purity O_2 (Matheson Tri-Gas) was used as received.

3. Results and Discussion

3.1. Low-Pressure ($\leq 1 \times 10^{-3}$ Torr) CO Adsorption. Up to CO pressures of 1×10^{-3} Torr, PM-IRAS measurements were carried out as follows: (1) cooling the preannealed AuPd(100) sample to ∼100 K, (2) leaking in purified CO to the designated pressures, and (3) stepwise warming the sample to the designated temperatures at which PM-IRAS spectra were acquired. Each spectrum was acquired for 300 scans at a resolution of 4 cm^{-1}.

Figure 1 displays typical spectra obtained at CO pressures of 1×10^{-7}, 1×10^{-5}, and 1×10^{-3} Torr. These spectra display similar trends; therefore, only the spectra in the left panel (CO pressure at 1×10^{-7} Torr) are described in detail. At 100 K, a strong CO band is apparent at 2108 cm^{-1} accompanied with a clear shoulder at ∼2085 cm^{-1}. With increasing temperature, the 2108 cm^{-1} feature gradually attenuates, blue shifts to higher frequencies, and finally diminishes at 220 K. In contrast, the ∼2085 cm^{-1} band remains rather constant until it disappears at ∼300 K. A new band at 2068 cm^{-1} develops at 180 K and then disappears at ∼300 K. It is noteworthy that the intensity of the 2085 cm^{-1} CO feature does not vary substantially with CO pressure nor is it very sensitive to the sample temperature. In contrast, the 2068 cm^{-1} band intensifies considerably with increasing CO pressure (its vibrational frequency also shifts to ∼2075 cm^{-1} at a CO pressure of 1×10^{-3} Torr) as seen from spectra displayed in the middle and right panels. The assignment of the band at $\nu_{CO} \geq 2108$ cm^{-1} to atop CO on Au sites is based on a number of previous studies regarding CO adsorption on various Au surfaces.[34−36] The most convincing evidence for this assignment is that this band blue shifts with decreasing CO coverage, common with Au but not Pd. This behavior has been suggested to be caused by the combination of a small positive dipolar component and a larger negative chemical shift component.[34] Both the 2085 and 2068 cm^{-1} bands are readily assigned to atop CO adsorbed on isolated Pd sites. This is based upon recent IRAS studies of CO adsorption on Mo(110)-supported Pd−Au alloy thin films[20,21] and oxide thin film supported Pd−Au particles.[37] More specifically, the 2085 cm^{-1} feature can be assigned to CO adsorbed on isolated surface Pd sites existing on the surface *prior to* CO adsorption while the 2068−2075 cm^{-1} band is assigned to CO adsorbed on isolated Pd sites that have segregated to the surface due to the presence of gas phase CO. It is important to note that at CO pressures $\leq 1 \times 10^{-3}$ Torr, a bridging CO band has never been observed on a well-annealed sample surface, neither by annealing the AuPd(100) sample from low to high temperatures nor by cooling from high to low temperatures.

Figure 2a plots the integrated CO IRAS signal areas as a function of sample temperature at CO pressures from 1×10^{-7} to 1×10^{-3} Torr; the bottom panel displays CO on Au sites and the upper panel CO on isolated Pd sites. For CO on Au sites, the IRAS signal area decreases almost linearly with increasing temperature at all CO pressures. It is also clear that higher CO pressure requires higher sample temperatures for CO to desorb. In contrast, CO adsorbed on isolated Pd sites displays distinct behavior, and the key findings are as follows: (1) Pd segregation only becomes apparent at sample temperatures above ∼200 K, suggesting near-surface Pd atoms only have limited mobility below this threshold temperature, and (2) higher CO pressures lead to enhanced Pd segregation to the surface. From the data shown in Figure 2a, temperatures at which the CO coverage reaches zero, i.e., temperatures at which the CO IRAS signal just becomes undetectable, are easily obtained. These values are used to calculate isosteric heats of adsorption of CO on both sites, and the plots are shown in Figure 2b. From these data the CO heat of adsorption at zero coverage on gold sites is found to be 69 kJ/mol, while that on isolated Pd sites is 84 kJ/mol. One should bear in mind that as the CO coverage increases, a decrease in the CO heat of adsorption is expected, due to repulsion between adjacent adsorbed CO molecules.[38] The CO heat of adsorption on Au single-crystal surfaces is typically very low, i.e., ∼50 kJ/mol on step sites and smaller than 40 kJ/mol on terrace sites.[34] In contrast, the CO heat of adsorption on Pd(100) is reported to be ∼153 kJ/mol.[38,39] Clearly, alloying causes an "averaging" of the CO binding

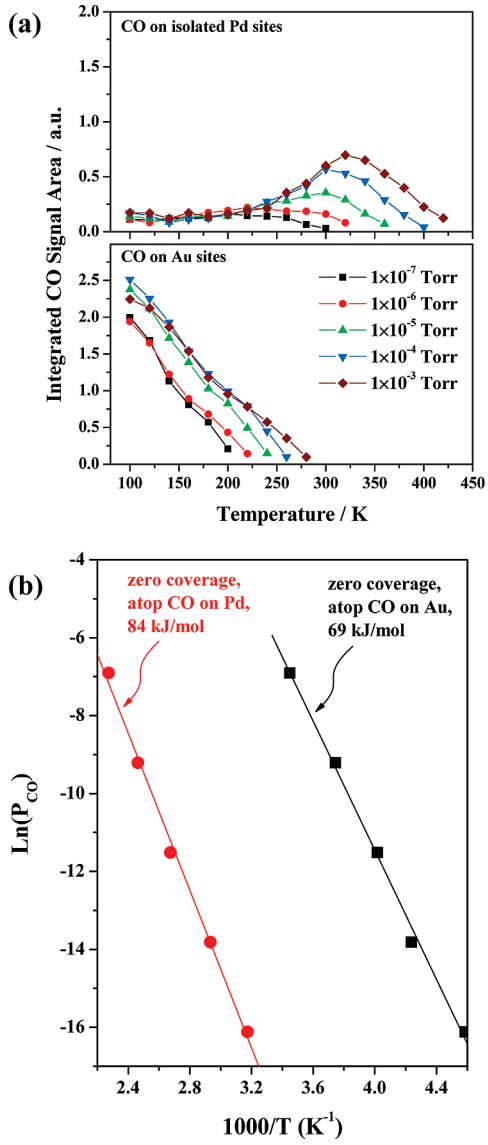

Figure 2. (a) Integrated CO PM-IRAS signal area as a function of sample temperature for CO on Au sites (lower panel) and isolated Pd sites (upper panel) at CO pressures of 1×10^{-7} (■), 1×10^{-6} (●), 1×10^{-5} (▲),1×10^{-4} (▼), and 1×10^{-3} (♦) Torr. (b) Isosteric plots of CO on Au sites (■) and isolated Pd sites (●).

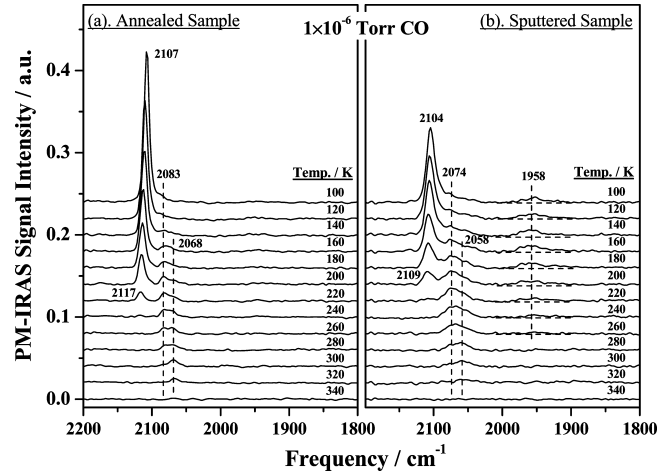

Figure 3. PM-IRAS spectra of CO on a well-annealed AuPd(100) sample (left) and a freshly ion-sputtered sample (right) at a CO pressure of 1×10^{-6} Torr as a function of sample temperature. Sample temperatures are marked adjacent to each spectrum.

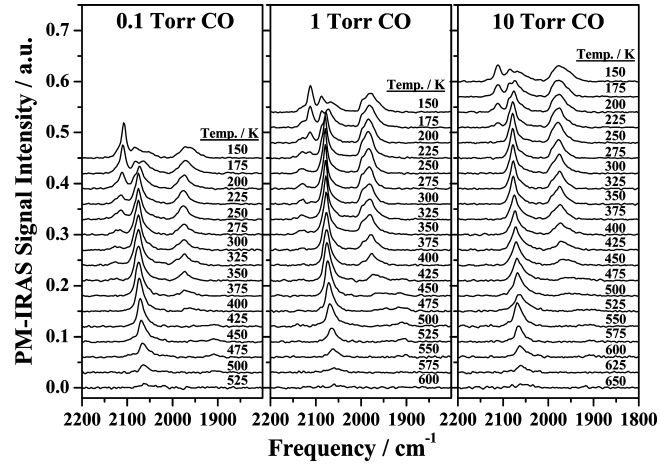

Figure 4. PM-IRAS spectra of CO on a well-annealed AuPd(100) sample as a function of temperature. Sample temperatures are marked adjacent to each spectrum. Spectra acquired at a CO pressure of (left) 0.1, (middle) 1, and (right) 10 Torr.

energy on both metals, presumably due to a ligand effect between the two metals.

As described earlier, no bridging CO has ever been found on a well-annealed AuPd(100) exposed to CO up to 1×10^{-3} Torr. However, bridging CO does appear on a freshly ion-sputtered sample (at room temperature, without annealing). IRAS spectra on annealed and sputtered samples were collected at a CO pressure of 1×10^{-6} Torr (Figure 3). Clear differences are noticed for the two surfaces: (1) regarding the signal intensity, CO on Au sites decreases while that on isolated Pd sites increases on the sputtered surface, consistent with more Pd being exposed by ion sputtering (note that the bulk composition of Pd and Au is 1:1); (2) regarding bandwidth, both bands broaden on the sputtered surface, due apparently to inhomogeneity of the sample surface caused by sputtering; and (3) more importantly, the appearance of an extra band centered at 1958 cm^{-1} demonstrates the presence of contiguous Pd sites.[20,21,37,40] It is important to point out that the CO binding energy on contiguous Pd sites is *lower* than that on isolated Pd sites, as evidenced by the fact that the 1958 cm^{-1} band disappears at lower temperatures compared with the band at 2083−2058 cm^{-1}. This behavior is also found at higher CO pressures and will be discussed in more detail below.

3.2. High-Pressure (≥0.1 Torr) CO Adsorption. At CO pressures higher than ~0.1 Torr, PM-IRAS spectra were obtained in a batch mode, where the AuPd(100) was first annealed to elevated temperatures after which CO was introduced and the PM-IRAS spectra acquired as the sample was stepwise cooled. Note that this strategy has been used successfully to obtain high-pressure CO IRAS spectra on Pd single crystals.[40] Figure 4 presents PM-IRAS spectra acquired at CO pressures of 0.1, 1, and 10 Torr at various sample temperatures. As assigned for CO spectra acquired at low pressures, the ν_{CO} at >2100 cm^{-1} corresponds to atop CO on Au sites and the ν_{CO} feature at 2060−2085 cm^{-1} to atop CO on isolated Pd sites.[20,21,37] The marked difference compared with CO at low pressures is the development of an intense band centered at ~1970 cm^{-1} as the sample is cooled. This feature is unambiguously assigned to bridging CO on contiguous Pd sites,[40,41] indicating significantly enhanced Pd segregation at elevated CO pressures. As expected, the higher the CO pressure, the higher the temperature at which the CO bands on isolated and contiguous Pd sites develop. However, this trend is no longer followed for CO

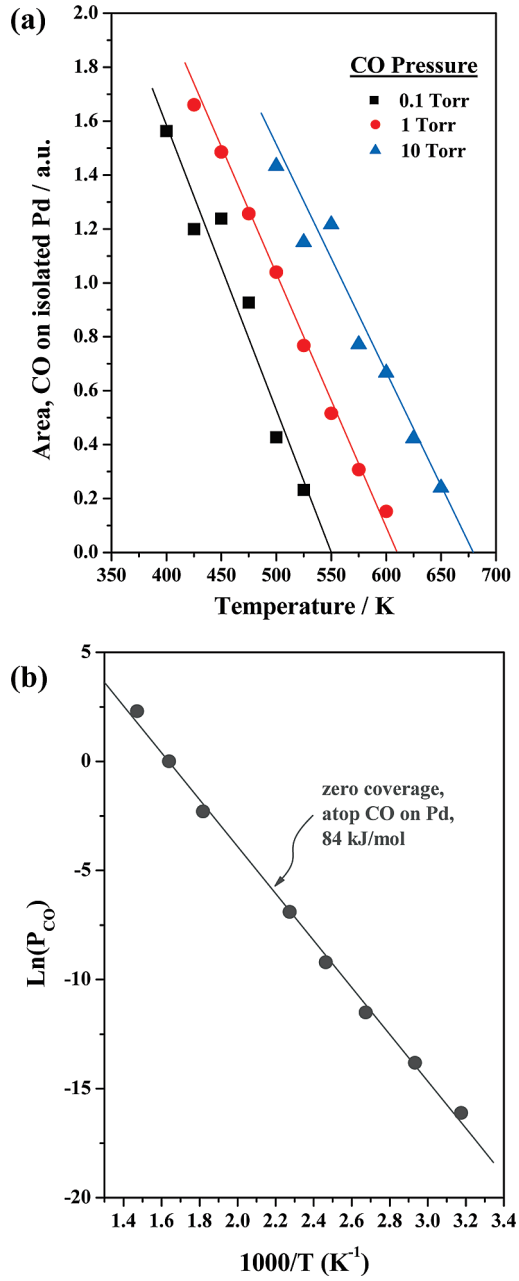

Figure 5. (a) Integrated CO PM-IRAS signal areas as a function of sample temperature for CO on isolated Pd sites at CO pressures of 0.1 (■), 1 (●), and 10 (▲) Torr. (b) Isosteric plots of CO on isolated Pd sites.

adsorbed on Au sites. For example, the CO band on Au sites develops at ~350 K at a CO pressure of 0.1 Torr, while this feature only appears at ~225 K in the presence of 10 Torr CO. This can only be rationalized by the existence of a source of contamination which becomes more severe at higher CO pressures and longer sampling time. The likely origin of this contamination is a hydrocarbon species originating from the inner wall of the high-pressure cell which can displace CO molecules and subsequently be irreversibly adsorbed at low sample temperatures. Nevertheless, the method used for acquisition of the PM-IRAS spectra, i.e., stepwise cooling the sample, suggests that CO adsorbed on isolated Pd sites is least perturbed by contamination since this band develops at the highest temperature. Figure 5a plots the integrated peak areas of this CO band as a function of temperature at the three CO pressures studied. Clearly, at relatively high sample temperatures, the signal area of this band decreases linearly with increasing temperature. The temperatures at which the CO coverage reaches zero are obtained straightforwardly from this graph. Note that the zero coverage temperatures of this band at lower CO pressures give an isosteric CO heat of adsorption of 84 kJ/mol (Figure 2b). As shown in Figure 5b, this behavior is readily extrapolated to higher CO pressures and an identical CO binding energy is obtained.

The surface free energy of Au (1.63 J/m^2 [42]) is substantially lower than that of Pd (2.05 J/m^2 [43]). Consequently, annealing an AuPd alloy in vacuum leads to Au segregation to the surface.[18−21] An alternative means of lowering the surface free energy is via adsorption.[22−27] The stronger interaction between CO and Pd causes Pd segregation to the surface. This study proves that higher CO pressures enhance Pd segregation. Although this is easy to understand, it is apparent from Figure 4 that the bridging CO band always develops at lower temperatures compared with the atop CO band on isolated Pd sites. The same is true for an ion-sputtered sample at low CO pressures (Figure 3b). This behavior proves that the CO binding energy on contiguous Pd sites is *lower* than that on isolated Pd sites, i.e., lower than 84 kJ/mol. In principle, the CO heat of adsorption on contiguous Pd sites can also be calculated isosterically. Surface contamination at elevated CO pressures, unfortunately, precludes a precise value to be obtained. Nevertheless, based on the PM-IRAS spectra shown in Figures 3b and 4, one can conclude that this energy lies between 69 and 84 kJ/mol. This is rather surprising since the CO binding energy on Pd(100) (where CO adsorbs solely on bridging sites) has been shown to be as high as 153 kJ/mol.[38,39] It is clear, therefore, that contiguous Pd sites on the surface of a AuPd alloy behave dramatically different from the surface of bulk Pd; this argues for a rather strong ligand effect between Au and Pd. In the following section, it is shown that this difference is profound for CO oxidation catalyzed by AuPd alloy surfaces.

3.3. CO Oxidation at Low Pressures ($P \leq 10^{-3}$ Torr). The reactivity for CO oxidation at low pressures ($\leq 10^{-3}$ Torr) was probed using a stoichiometric CO + O_2 mixture in a steady-state flow mode.[30−32] The reactants were leaked into the chamber, and the unreacted reactants and the CO_2 product were monitored simultaneously with a mass spectrometer (QMS). For a well-annealed AuPd(100) surface without contiguous Pd sites, the 44 amu (CO_2) QMS signal intensity never becomes higher than the background, i.e., no CO_2 formation is found for any reaction conditions. Note that at CO pressures $\leq 10^{-3}$ Torr, we demonstrated in section 3.1 that Pd segregation never becomes sufficiently extensive to form contiguous Pd sites on the surface. Since CO does indeed adsorb on the alloy surface during reaction, the lack of CO_2 production proves unambiguously that neither Au nor isolated Pd sites are capable of dissociating O_2.[28] This notion is further corroborated by experiments carried out on a freshly ion-sputtered surface (without annealing). CO_2 formation indeed occurs as low as ~160 K using such a surface, and CO titration does reveal the existence of contiguous Pd sites on this surface (Figure 3). However, it is not entirely appropriate to draw firm conclusions using an ion-sputtered sample since reaction may very well occur on defect sites created during the sputtering process. More convincing evidence will be shown below regarding the importance of contiguous Pd sites for CO oxidation at elevated pressures.

3.4. CO Oxidation at High Pressures ($P > 0.1$ Torr). Note first that at CO pressures higher than ~0.1 Torr, extensive Pd segregation occurs such that contiguous Pd sites form on the AuPd(100) surface (Figure 4). O_2 dissociation occurs on these

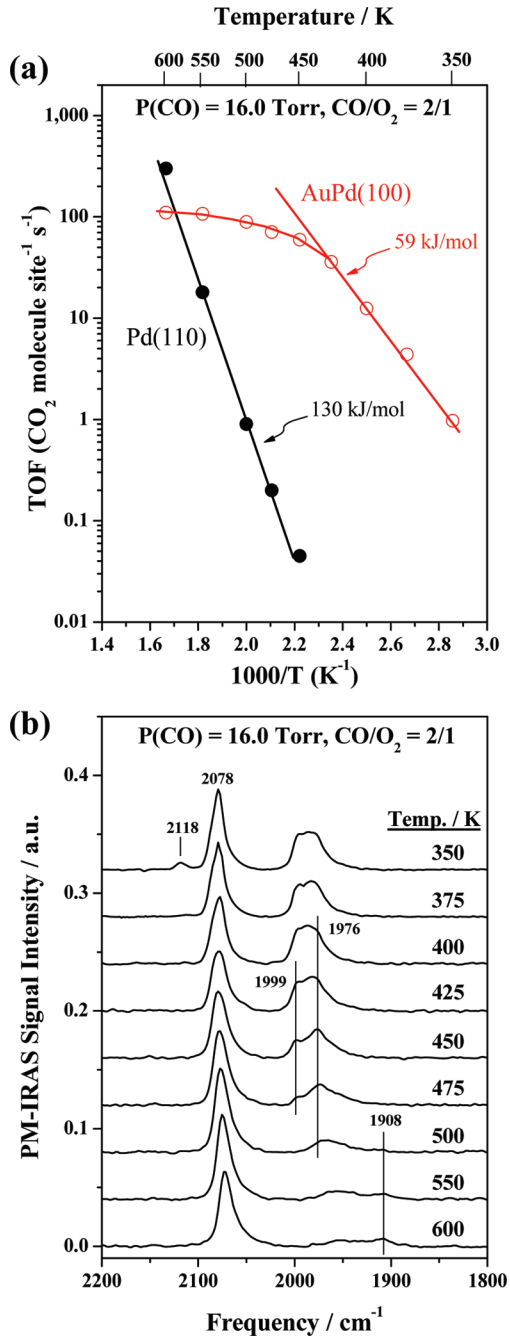

Figure 6. (a) Arrhenius plots of CO_2 formation rate (in TOF) over AuPd(100) and Pd(110) (kinetic data for Pd(110) are taken from ref 44) with 16 Torr CO and 8 Torr O_2. (b) Corresponding PM-IRAS spectra acquired at the reaction temperatures marked adjacent to each spectrum.

sites, and CO oxidation proceeds promptly at ambient temperatures.[28] In the following the reaction kinetics is probed in more detail. Figure 6a shows the CO_2 formation rate (presented as turnover frequency, i.e., CO_2 molecules per metal site per second) versus temperature over AuPd(100) in Arrhenius form. Since surface composition changes with temperature and reactant total pressure and composition (see below), the surface Pd/Au ratio at any given reaction condition is difficult to obtain. Since both surface Pd and Au participate in CO oxidation, the total surface atom density is taken to be the same as Pd(100): 1.33×10^{15} cm^{-2}.[38] This is reasonable since the lattice mismatch between Pd and Au is rather small (~4.9%).[44] For comparison, kinetic data using Pd(110) are also shown under the same gas pressure and composition (CO pressure 16 Torr, $CO/O_2 = 2/1$) conditions.[45] The key finding here is that AuPd(100) shows significantly higher reactivity at low temperatures compared with a Pd single crystal. For instance, the CO_2 formation rate at 450 K over AuPd(100) is $\sim 10^3$ times higher than that over Pd(110). At lower temperatures the difference is even more significant. These results demonstrate that CO inhibition, the factor that causes low reactivity of pure Pd at low temperatures,[30−32,45−47] does not occur with AuPd(100). This behavior is fully consistent with the considerably reduced binding energy of CO with AuPd(100) compared with pure Pd. The isosteric heat of adsorption of CO on isolated Pd site is 84 kJ/mol and on Au sites 69 kJ/mol (Figure 2b); on contiguous Pd site the value lies somewhere between these two values (Figures 3 and 4). Note that the binding energy of CO on Pd(100) is ~153 kJ/mol.[38,39] This large difference in CO binding energies on these two surfaces appears to be a key point in explaining the marked difference in low-temperature CO oxidation activity, i.e., the low binding energy between CO and AuPd(100) allows facile CO desorption even near room temperature as well as O_2 adsorption and dissociation, an exceedingly slow combined process on pure Pd at such temperatures. Figure 6b presents the corresponding PM-IRAS spectra at various reaction temperatures. It should be mentioned first that contamination is no longer an issue even at high pressure and extended sampling times for the CO + O_2 mixtures. This is believed to be due to the fact that hydrocarbon contaminants are easily oxidized by oxygen. Note first that the atop CO band on Au sites (~2118 cm^{-1}) is only detectable at 350 K, consistent with the lowest binding of CO with Au. There are at least three bridging CO features on contiguous Pd sites at ~1999, ~1976, and ~1908 cm^{-1}, demonstrating the inhomogeneity of the contiguous Pd ensembles. Note that (1) below ~425 K the bridging CO band intensity persists and decreases at higher temperatures and (2) the signal intensity of the atop CO band on isolated Pd sites at ~2078 cm^{-1} remains rather constant to 600 K. This behavior is fully consistent with the higher CO binding energy of CO on isolated Pd compared with contiguous Pd sites derived with pure CO (Figure 4).

It is further noticed from Figure 6a that from 350 to 425 K the CO_2 formation rate increases linearly with temperature over AuPd(100). The analogous situation for pure Pd has been studied in great detail, and the reaction mechanism is rather well understood. For pure Pd the surface is predominantly covered by adsorbed CO in this linear regime, and as such, the reaction rate is limited by the rate at which desorption of CO opens adsorption/dissociation surface sites for incoming O_2. The measured reaction kinetics at reducing or mildly oxidizing conditions support this mechanistic picture in exhibiting first-order dependence on O_2 pressure and a negative first-order dependence on CO pressure. Furthermore, the apparent activation energy for CO_2 formation is approximately equal to the CO desorption energy.[30−32,45−47] On the basis of these studies, we propose that the same mechanism is applicable to AuPd(100) below ~425 K, i.e., the surface is predominantly covered with CO and the reaction rate determined by CO desorption. This notion is corroborated by two findings: (1) the sample is indeed fully covered with CO below ~425 K (Figure 6b) and (2) the apparent reaction activation energy (59 kJ/mol) is indeed close to the CO binding energies (Figure 2b). In contrast, the reaction rate "rollover" above 425 K is more difficult to rationalize due to the simple fact that the surface composition (Pd/Au ratio and distribution) varies with temperature. There are at least two possibilities to explain this behavior: (1) the residence time of

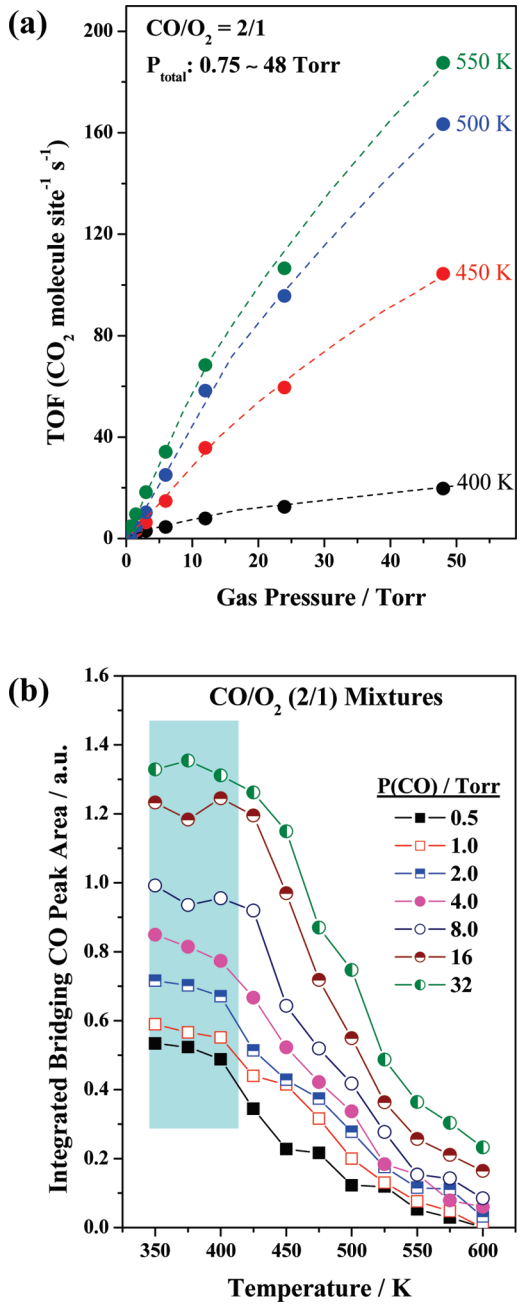

Figure 7. (a) CO_2 formation rates (TOF) as a function of reactant pressure at 400, 450, 500, and 550 K with a CO/O_2 (2/1) mixture and total pressures varying from 0.75 to 48 Torr. (b) Integrated bridging CO peak areas versus reaction temperature. Note that the shaded area indicates that below ~400 K the surfaces are saturated with CO.

CO on Au sites becomes too short at high temperatures, even though CO molecules adsorbed on Au sites are likely the most reactive due to their weakest binding with the surface, and (2) the density of contiguous Pd sites decreases with increasing temperature (Au tends to diffuse back to the surface with an increase in temperature). Note that O_2 dissociation occurs exclusively on these sites.

To elucidate the reaction in further detail, kinetic measurements were performed using stoichiometric reactants (CO/O_2 = 2/1) at various total pressures. Such experiments are especially useful in determining which surface sites are more important in CO_2 formation, since the surface Pd/Au ratio can be easily tuned by varying the total reactant pressure. Figure 7a displays the CO_2 formation rate as a function of reactant pressure at four reaction temperatures (data at 400 K have been reported elsewhere[28]). A general trend follows at all reaction temperatures, that is, the reaction rate increases with increasing gas pressure at the conditions investigated. In situ PM-IRAS spectra[28] have revealed that this is due to the fact that more Pd atoms are segregated to the surface as the reactant pressure increases such that the contiguous Pd site (where O_2 dissociation occurs) density increases. The number of contiguous Pd sites, even though difficult to determine quantitatively, can be qualitatively determined from the bridging CO peak areas. Figure 7b displays the integrated bridging CO peak areas as a function of temperature for CO/O_2 (2/1) mixtures where the CO pressure is varied from 0.5 to 32 Torr. Below ~400 K the CO signal area remains essentially constant (marked area) at all CO pressures investigated, demonstrating that the surface is saturated with CO. As such, the CO signal area provides a qualitative measure of the number of contiguous Pd sites. Above ~400 K the situation becomes more complex since the drop in signal area can be explained by a combination of effects: (1) desorption of CO and (2) a decrease in the number of contiguous Pd sites due to Au diffusion to the surface. In any case, there is clear evidence that CO adsorbed on Au and isolated Pd sites also participates in oxidation. As displayed in Figure 7b, the number of contiguous Pd sites increases ~2−3 times as the CO pressure increases from 0.5 to 32 Torr, while the kinetic data shown in Figure 7a reveal that the reaction rate increases by orders of magnitude during the pressure increase. This is rationalized by the fact that the higher gas pressures enhance the CO population on Au and isolated Pd sites (especially Au sites, where the CO binding energy is the lowest) and that these CO molecules, in turn, participate in the overall reaction.[28] This is presumably achieved by $O_{(ads)}$ spillover, since $O_{(ads)}$ is formed exclusively on contiguous Pd sites.

Finally, the structure−reactivity relationship is further probed by varying the CO/O_2 ratio of the reactants. This also allows the determination of which reactant, CO or O_2, is more responsible for Pd segregation. The experiments were performed by maintaining CO (or O_2) at 8 Torr while varying O_2 (or CO) from 0.5 to 64 Torr. Reactions were carried at two temperatures, 400 and 550 K. As displayed in the left panel of Figure 8a, by maintaining 8 Torr of CO, the reaction is +1 order in O_2 for O_2 pressures ≤4 Torr and −0.4 order in O_2 at higher O_2 pressures. In contrast, by maintaining 8 Torr of O_2, the kinetic data show an order of +0.5 in CO for CO pressures ≤16 Torr. The reaction is still positive order in CO pressure even when it is as high as 64 Torr. At similar pressures (the temperature must be much higher in order to have measurable rates), this reaction is +1 order in O_2 pressure and −1 order in CO pressure over pure Pd.[48] Again, the surface composition and distribution for AuPd(100) vary with varying reactants, making quantitative analysis impossible. Nevertheless, this dramatic difference between pure Pd and the AuPd alloy can be interpreted, at least qualitatively, as due to the considerable difference in the CO binding energy. Figure 8b presents the corresponding in situ PM-IRAS spectra. It is inferred from these spectra (at 400 K the surfaces should be saturated with CO, see Figure 7b) that CO is the dominant species that induces Pd segregation, i.e., by maintaining the CO pressure, the CO signal area is essentially retained (left) while an increase in the CO pressure leads to an increase in the bridging CO peak area (right). The combination of the kinetics and PM-IRAS spectra suggests that the relatively low binding energy of CO with the alloy surface prevents

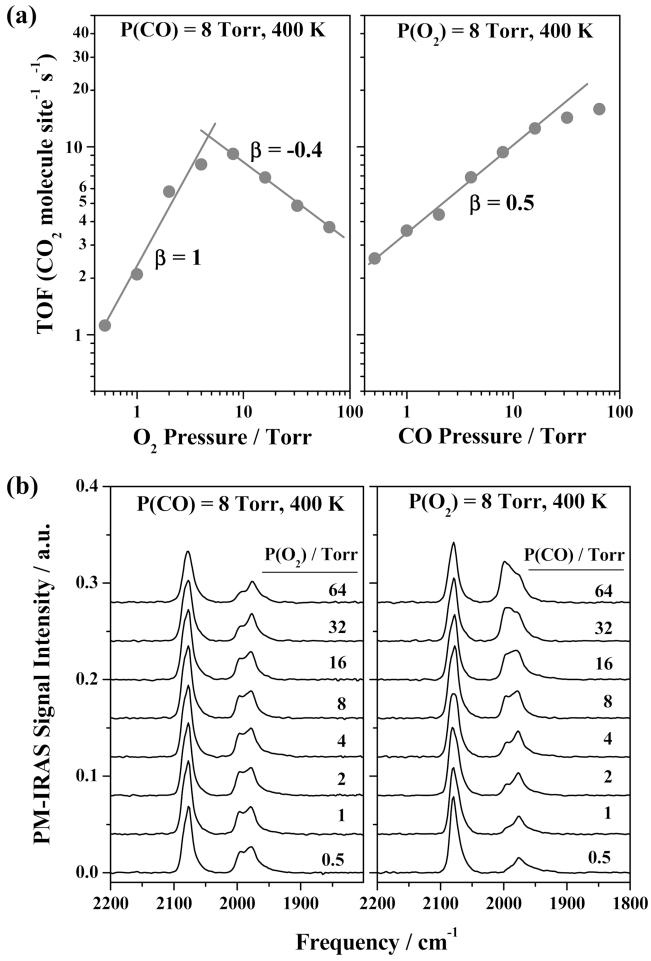

Figure 8. (a) CO_2 formation rate (TOF) at 400 K using 8 Torr CO and various pressures of O_2 (from 0.5 to 64 Torr) (left) and 8 Torr O_2 and various pressures of CO (from 0.5 to 64 Torr) (right). (b) Corresponding PM-IRAS spectra using 8 Torr CO and various pressures of O_2 (from 0.5 to 64 Torr) (left) and 8 Torr O_2 and various pressures of CO (from 0.5 to 64 Torr) (right).

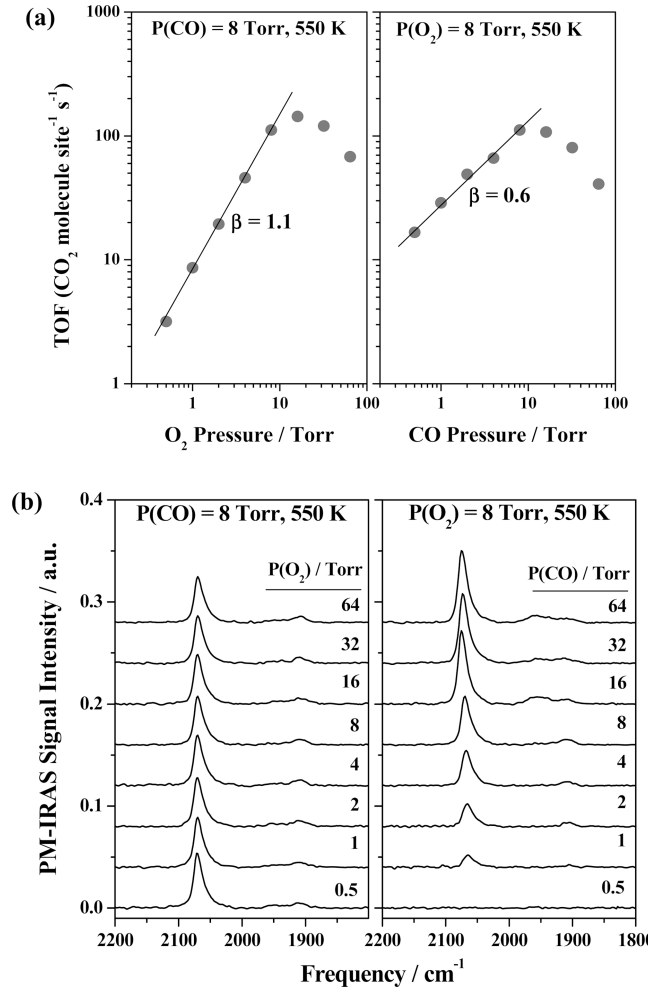

Figure 9. (a) CO_2 formation rate (TOF) at 550 K using 8 Torr CO and various pressures of O_2 (from 0.5 to 64 Torr) (left) and 8 Torr O_2 and various pressures of CO (from 0.5 to 64 Torr) (right). (b) Corresponding PM-IRAS spectra using 8 Torr CO and various pressures of O_2 (from 0.5 to 64 Torr) (left) and 8 Torr O_2 and various pressures of CO (from 0.5 to 64 Torr) (right).

inhibition of the reaction by CO at increasing CO pressures. On the contrary, CO induces Pd segregation and promotes the reaction.

Identical experiments were carried out at 550 K, and the kinetic data and PM-IRAS spectra are shown in Figure 9a and 9b, respectively. Note first that at this reaction temperature the surfaces are no longer fully covered with CO, especially contiguous Pd sites. In this case, the reaction rate is likely determined by the surface coverages of $CO_{(ads)}$ and $O_{(ads)}$. This is consistent with the fact that the CO_2 formation rate decreases when the CO (or O_2) pressure is in great excess to that of O_2 (or CO). The reaction rate decrease (shown in the left panel of Figure 8a) at high O_2 pressures at 400 K may also be interpreted in the same fashion. Finally, it is noted that at 550 K and rather high O_2/CO ratios (up to 8/1) there is no evidence of Pd oxidation occurring with the AuPd(100) sample. For Pd single crystals under similar conditions, Pd oxidation occurs as evidenced by the appearance of CO bands (at ~2142 cm^{-1}) that are characteristic of adsorption on an oxidized phase.[31] As displayed in the left panel of Figure 9b, no such bands are observed, indicating that the surface Pd remains reduced. This behavior, i.e., Pd in a AuPd alloy is more difficult to oxidize, can be rationalized using simple electronegativity arguments. The electronegativity of Pd (2.20) is less than Au (2.54), suggesting electron transfer from Pd to Au, causing Pd to be more difficult to oxidize.[49]

3.5. Implications. Finally, the impact of this study to important industrial processes, e.g., vinyl acetate (VA) synthesis and catalytic emission conversion, is briefly addressed. VA synthesis, i.e., $C_2H_4 + CH_3COOH + 1/2O_2 \rightarrow CH_3COOCH{=}CH_2 + H_2O$, is commercially catalyzed by Pd−Au alloys.[1−12] Total combustion of reactants (ethylene and acetic acid) is the side reaction that causes the VA selectivity to decrease; CO oxidation is the final step of these combustion reactions. This implies that by decreasing the number of contiguous Pd sites, this reaction pathway can be blocked and, correspondingly, the VA selectivity enhanced. Indeed, properly distributed isolated Pd sites were found to be the catalytically active sites for the reaction.[10] On the other hand, O_2 activation, the rate-determining step in VA synthesis at elevated pressures,[8,9] cannot occur without contiguous Pd sites as shown in the current study. The combination of both factors indicates that the total combustion pathway during VA synthesis cannot be completely eliminated. In other words, 100% selectivity in VA synthesis is not achievable using Pd−Au alloy catalysts. Currently VA selectivity of ~92% is realized using commercial Pd−Au alloy catalysts.[50] This is consistent with our conclusion and implies that there is little margin for further improvement of the commercial catalysts in VA synthesis.

This study also has shown and rationalizes the low-temperature CO oxidation activity of a AuPd alloy. In light of the recent U.S. patents[17] that utilize AuPd alloy under realistic conditions, these data suggest great potential of this system for application as a three-way catalytic converter (TWC). In particular, the emission problem that typically occurs during cold start can very likely be avoided using a AuPd alloy catalyst.

4. Conclusions

PM-IRAS has been used to study CO adsorption on a AuPd(100) surface over a wide range of CO pressures from 1×10^{-7} to 10 Torr on well-annealed and freshly ion-sputtered surfaces. At CO pressures lower than $\sim 1 \times 10^{-3}$ Torr, Pd segregation to the surface is found as evidenced by the enhanced CO band intensity on isolated Pd sites with increasing CO pressure. However, the extent of segregation never becomes sufficient to form contiguous Pd sites on a well-annealed sample surface. At CO pressures higher than ~0.1 Torr, Pd segregation is enhanced such that contiguous Pd sites are formed. Isosteric heats of adsorption of CO on Au sites and isolated Pd sites are 69 and 84 kJ/mol, respectively. It is also found that the binding energy of CO on contiguous Pd sites is lower than that on isolated Pd sites. For CO oxidation the key findings are the following: (1) contiguous Pd sites are critical, the role of which is to dissociate O_2 and provide atomic oxygen for the reaction, and (2) reaction kinetic measurements indicate that reaction is carried out on contiguous Pd sites, Au sites, or even isolated Pd sites. $O_{(ads)}$ generated at contiguous Pd sites "spills over" to Au/isolated Pd sites to react with chemisorbed CO. This work implies that low-temperature CO oxidation should occur facilely on supported Au−Pd alloy particles and that particle size and support effects should be much less critical for Au−Pd alloy catalysts compared with supported, Au-only catalysts.

Acknowledgment. We gratefully acknowledge the support for this work by the Department of Energy, Office of Basic Energy Sciences, Division of Chemical Sciences, Geosciences, and Biosciences (DE-FG02-95ER-14511), and the Robert A. Welch Foundation.

References and Notes

(1) Allison, E. G.; Bond, G. C. *Catal. Rev.* **1972**, *7*, 233.
(2) Nakamura, S.; Yasui, T. *J. Catal.* **1970**, *17*, 366.
(3) Samanos, B.; Boutry, P. *J. Catal.* **1971**, *23*, 19.
(4) Provine, W. D.; Mills, P. L.; Lerou, J. J. *Stud. Surf. Sci. Catal.* **1996**, *101*, 191.
(5) Macleod, N.; Keel, J. M.; Lambert, R. M. *Appl. Catal., A* **2004**, *261*, 37.
(6) Han, Y. F.; Kumar, D.; Goodman, D. W. *J. Catal.* **2005**, *230*, 353.
(7) Stacchiola, D.; Calaza, F.; Burkholder, L.; Tysoe, W. T. *J. Am. Chem. Soc.* **2004**, *126*, 15384.
(8) Han, Y. F.; Kumar, D.; Sivadinarayana, C.; Goodman, D. W. *J. Catal.* **2004**, *224*, 60.
(9) Han, Y. F.; Wang, J. H.; Kumar, D.; Yan, Z.; Goodman, D. W. *J. Catal.* **2005**, *232*, 467.
(10) Chen, M. S.; Kumar, D.; Yi, C. W.; Goodman, D. W. *Science* **2005**, *310*, 291.
(11) Kumar, D.; Han, Y. F.; Chen, M. S.; Goodman, D. W. *Catal. Lett.* **2006**, *106*, 1.
(12) Chen, M. S.; Luo, K.; Wei, T.; Yan, Z.; Kumar, D.; Yi, C. W.; Goodman, D. W. *Catal. Today* **2006**, *117*, 37.
(13) Piccolo, L.; Piednoir, A.; Bertolini, J. C. *Surf. Sci.* **2005**, *592*, 169.
(14) Dimitratos, N.; Villa, A.; Wang, D.; Porta, F.; Su, D.; Prati, L. *J. Catal.* **2006**, *244*, 113.
(15) Enache, D. I.; Edwards, J. K.; Landon, P.; Solosona-Espriu, B.; Carley, A. F.; Herzing, A. A.; Watanabe, M.; Kiely, C. J.; Knight, D. W.; Hutchings, G. J. *Science* **2006**, *311*, 362.
(16) Landon, P.; Collier, P. J.; Papworth, A. J.; Kiely, C. J.; Hutchings, G. J. *Chem. Commun.* **2002**, *18*, 2058.
(17) Fujdala, K. L. ; Truex, T. J. U.S. Patents 20080125308, 20080125313, 20080124514.
(18) Li, Z.; Gao, F.; Wang, Y.; Calaza, F.; Burkholder, L.; Tysoe, W. T. *Surf. Sci.* **2007**, *601*, 1898.
(19) Li, Z.; Furlong, O.; Calaza, F.; Burkholder, L.; Poon, H. C.; Saldin, D.; Tysoe, W. T. *Surf. Sci.* **2008**, *602*, 1084.
(20) Yi, C. W.; Luo, K.; Wei, T.; Goodman, D. W. *J. Phys. Chem. B* **2005**, *109*, 18535.
(21) Wei, T.; Wang, J.; Goodman, D. W. *J. Phys. Chem. C* **2007**, *111*, 8781.
(22) Nerlov, J.; Chorkendorff, I. *J. Catal.* **1999**, *181*, 271.
(23) Nerlov, J.; Sckerl, S.; Wambach, J.; Chorkendorff, I. *Appl. Catal., A* **2000**, *191*, 97.
(24) Christoffersen, E.; Stoltze, P.; Nøskov, J. K. *Surf. Sci.* **2002**, *505*, 200.
(25) Hirsimäki, M.; Lampimäki, M.; Lahtonen, K.; Chorkendorff, I.; Valden, M. *Surf. Sci.* **2005**, *583*, 157.
(26) Gonzalez, S.; Neyman, K. M.; Shaikhutdinov, S.; Freund, H. J.; Illas, F. *J. Phys. Chem. C* **2007**, *111*, 6852.
(27) Tao, F.; Grass, M. E.; Zhang, Y.; Butcher, D. R.; Renzas, J. R.; Liu, Z.; Chung, J. Y.; Mun, B. S.; Salmeron, M.; Somorjai, G. A. *Science* **2008**, *322*, 932.
(28) Gao, F.; Wang, Y.; Goodman, D. W. *J. Am. Chem. Soc.* **2009**, *131*, 5734.
(29) Piednoir, A.; Languille, M. A.; Piccolo, L.; Valcarcel, A.; Cadete Santos. Aires, F. J.; Bertolini, J. C. *Catal. Lett.* **2007**, *114*, 110.
(30) Gao, F.; McClure, S. M.; Cai, Y.; Gath, K. K.; Wang, Y.; Chen, M. S.; Guo, Q. L.; Goodman, D. W. *Surf. Sci.* **2009**, *603*, 65.
(31) Gao, F.; Wang, Y.; Cai, Y.; Goodman, D. W. *J. Phys. Chem. C* **2009**, *113*, 174.
(32) Gao, F.; Cai, Y.; Gath, K. K.; Wang, Y.; Chen, M. S.; Guo, Q. L.; Goodman, D. W. *J. Phys. Chem. C* **2009**, *113*, 182.
(33) Han, P.; Axnanda, S.; Lyubinetsky, I.; Goodman, D. W. *J. Am. Chem. Soc.* **2007**, *129*, 14355.
(34) Kim, J.; Samano, E.; Koel, B. E. *J. Phys. Chem. B* **2006**, *110*, 17512.
(35) Meier, D. C.; Goodman, D. W. *J. Am. Chem. Soc.* **2004**, *126*, 1892.
(36) Lemire, C.; Meyer, R.; Shaikhutdinov, S. K.; Freund, H. J. *Surf. Sci.* **2004**, *552*, 27.
(37) Luo, K.; Wei, T.; Yi, C. W.; Axnanda, S.; Goodman, D. W. *J. Phys. Chem. B* **2005**, *109*, 23517.
(38) Engel, T.; Ertl, G. *Adv. Catal.* **1979**, *28*, 1.
(39) Conrad, H.; Ertl, G.; Koch, J.; Latta, E. E. *Surf. Sci.* **1974**, *43*, 462.
(40) Szanyi, J.; Kuhn, W. K.; Goodman, D. W. *J. Vac. Sci. Technol. A* **1993**, *11*, 1969.
(41) Mazzone, G.; Rivalta, I.; Russo, N.; Sicilia, E. *J. Phys. Chem. C* **2008**, *112*, 6073.
(42) Tyson, W. R.; Miller, W. A. *Surf. Sci.* **1977**, *62*, 267.
(43) Mezey, L. Z.; Giber, J. *Jpn. J. Appl. Phys.* **1982**, *11*, 1569.
(44) Banhart, B. *Phys. Rev. B* **1996**, *53*, 7128.
(45) Berlowitz, P. J.; Peden, C. H. F.; Goodman, D. W. *J. Phys. Chem.* **1988**, *92*, 5213.
(46) Szanyi, J.; Goodman, D. W. *J. Phys. Chem. B* **1994**, *98*, 2972.
(47) Szanyi, J.; Goodman, D. W. *J. Phys. Chem. B* **1994**, *98*, 2978.
(48) Xu, X.; Goodman, D. W. *J. Phys. Chem.* **1993**, *97*, 7711.
(49) Kotsifa, A.; Halkides, T. I.; Kondarides, D. I.; Verykios, X. E. *Catal. Lett.* **2002**, *79*, 113.
(50) *Catal. Gold News* **2003**, *4* (Spring).

JP9053132